JOURNAL OF MATERIALS SCIENCE 29 (1994) 809–815

Physical and electrical properties of MnO_2-doped $Pb(Zr_xTi_{1-x})O_3$ ceramics

JONG SUN KIM*, KI HYUN YOON
Department of Ceramic Engineering, Yonsei University, Seoul, Korea

The effects of composition on the physical property change in the phase coexistence region between the tetragonal and rhombohedral phases have been investigated as a function of zirconium concentration, x, for the MnO_2-doped $Pb(Zr_xTi_{1-x})O_3$ ($0.40 \leqslant x \leqslant 0.60$) ceramics. The relative amount of phase coexisting between the tetragonal and rhombohedral phases affects greatly both dielectric and piezoelectric properties as a function of zirconium concentration. However, there are no detectable changes between the apparent density and microstructure. Also, in the coexistence region, the relative amount of coexistence of the rhombohedral phase increases with MnO_2 addition. The inflection points of the dielectric constant shift to lower zirconium concentration in proportion to the MnO_2 addition, owing to the substitution effect on the PZT lattice site.

1. Introduction

$Pb(Zr_xTi_{1-x})O_3$ solid solutions are excellent piezoelectric materials owing to their morphotropic phase-boundary properties. The region of phase transition between the tetragonal and rhombohedral structures in the $Pb(Zr_xTi_{1-x})O_3$ ceramics shows very adaptable piezoelectric characteristics due to the phase coexistence phenomena and exhibits a sensitivity of properties to the preparation methods, the composition, the kinds of additives, the firing temperatures, and the external electrical and mechanical stresses [1–5].

The understanding of the relationships between variations in physical properties and phase coexistence with composition is very important because it produces a great influence on the characteristics of the PZT ceramics and stabilities with temperature and time in the region of the phase transition between the tetragonal and rhombohedral phases.

Therefore, in this work, the phase coexistence phenomena for the $Pb(Zr_xTi_{1-x})O_3$ ($0.40 \leqslant x \leqslant 0.60$) ceramics with variations of MnO_2 additive and zirconium concentration were investigated. In addition, the dielectric and piezoelectric properties with change in composition and microstructure have been discussed.

2. Experimental procedure

The $Pb(Zr_xTi_{1-x})O_3$ ceramics in the composition range $x = 0.40$–0.60 at intervals of 2 mol %, were prepared by employing the usual ceramic fabrication technique. In addition, $Pb(Zr_xTi_{1-x})O_3$ was doped with 0.0–2.0 wt % MnO_2 to investigate the effect of the inhomogeneous distribution of the MnO_2 additive [6, 7].

In conventionally prepared PZT ceramics with compositions near the morphotropic phase boundary (MPB), the tetragonal and the rhombohedral phases always coexist [8]. The width and properties of the coexistence region are associated with the occurrence of compositional fluctuation of Ti^{4+} and Zr^{4+} ions in the PZT materials [2, 8]. Compositional fluctuation due to a non-uniform distribution of titanium and zirconium ions leads to a broad variation in dielectric constant with zirconium concentration in the MPB region [1, 8]. The width of this coexistence region and the structure of PZT ceramics are greatly affected by the firing time and temperature [9]. Thus, in this work, to minimize the compositional fluctuation effect, the PZT ceramics were synthesized and sintered under carefully controlled conditions, as follows. The raw materials used were 99% pure PbO (Litharge; Shinyo Pure Chemicals), 99.9% pure ZrO_2 (Baddeleyite; Junsei Chemicals), 99% pure TiO_2 (Anatase; Fluka AG), and 99% pure MnO_2 (Fluka AG). Raw materials were weighed into 20 g batches for each given composition and wet-milled for 12 h, with ZrO_2 grinding media in ethyl alcohol. The mixed slurries were dried, and then the PZT powders were synthesized by calcination at 850 °C for 6 h in an alumina crucible.

The PZT powders after granulation were pressed under 1500 kg cm^{-2} into pellets 14 mm diameter. The pellets were placed in a specially arranged alumina crucible and sintered in an electric furnace at a temperature of 1200 °C for 4 h with a heating rate of 300 °C h^{-1}. The $PbZrO_3$ + 5.0 wt % ZrO_2 mixtures were used for the PbO atmosphere buffer powders. The density and water absorption of the sintered specimens were measured.

The fired specimens were lapped step-by-step with SiC papers (nos 800, 1000, 1200) to 0.5 mm thickness. The specimens were cleaned with ethanol and distilled

* *Present address*: R and D Centre, Samsung Corning Company Ltd, Gumi, Korea.

water using an ultrasonic cleaner. After lapping, the silver paste was printed, and then fired, on to the faces at 700 °C for 10 min for poling treatment and properties measurement. An LCR meter (Ando Electric Co., AG4303) was used to measure the dielectric constant and tan δ of the specimens. The electroded specimens were poled in silicone oil at 100 °C by applying a high d.c. field of 10–30 kV cm^{-1} for 20 min and field-cooled to room temperature. The planar coupling constant was measured by a method similar to that of the IRE Standard [6].

The lattice parameters of each specimen were determined by the least square method with an X-ray diffractometer (Rigaku Co., Japan). The (2 0 0) reflections of the X-ray diffraction patterns for the PZT solid solutions can be selected to study phase coexistence in the phase-transition region because they show strong intensity and peak separation, as reported by Hahn *et al.* [10] and Mabud [9]. They split into two for the tetragonal structure, but do not split for the rhombohedral structure; They give three lines in the solid solutions containing both structures. Thus, the relative amount of rhombohedral phase in the phase coexistence regions can be calculated from Equation 1.

relative amount of rhombohedral phase =

$$I_{(2\,0\,0)r}/(I_{(2\,0\,0)t} + I_{(2\,0\,0)r} + I_{(0\,0\,2)t}) \qquad (1)$$

where $I_{(2\,0\,0)t}$ and $I_{(0\,0\,2)t}$ are the intensities of the (2 0 0) and (0 0 2) reflection lines of the tetragonal phase, and $I_{(2\,0\,0)r}$ is that of the (2 0 0) reflection line of the rhombohedral phase.

Microstructures were examined by the optical microscope (Nikon, type 104, Japan) and SEM (Jeol, JXA-840A) for the polished and chemically etched surfaces of the specimens. Also, the *D–E* hysteresis loop characteristics were measured by using the Sawyer–Tower circuit.

3. Results and discussion

Fig. 1 shows variation in pattern of the (2 0 0) reflection in the MnO_2-doped $Pb(Zr_{0.52}Ti_{0.48})O_3$ ceramics. The tendency of pattern variation with increasing MnO_2 addition shows slightly single broad peaks. As reported by Weston *et al.* [11], this indicates variation of the coexistence state between the tetragonal and rhombohedral phases with increasing MnO_2 addition. Ouchi *et al.* [12] also reported that the morphotropic boundary between the tetragonal and rhombohedral phases was shifted slightly to the tetragonal region when MnO_2 was added to the $Pb(Mg_{1/3}Nb_{2/3})O_3$–$PbZrO_3$–$PbTiO_3$ ternary solid-solution system.

Fig. 2 shows the variation of $I_{(2\,0\,0)r}/(I_{(0\,0\,2)t} + I_{(2\,0\,0)r} + I_{(2\,0\,0)t})$ ratio for the (2 0 0) reflection which means the relative amount of the rhombohedral phase in the phase coexistence region, as reported by Hahn *et al.* [10] and Mabud [13]. As the amount of MnO_2 addition increases, the coexisting amount of the rhombohedral phase initially increases up to 0.5 wt % MnO_2 addition, and then slightly saturates.

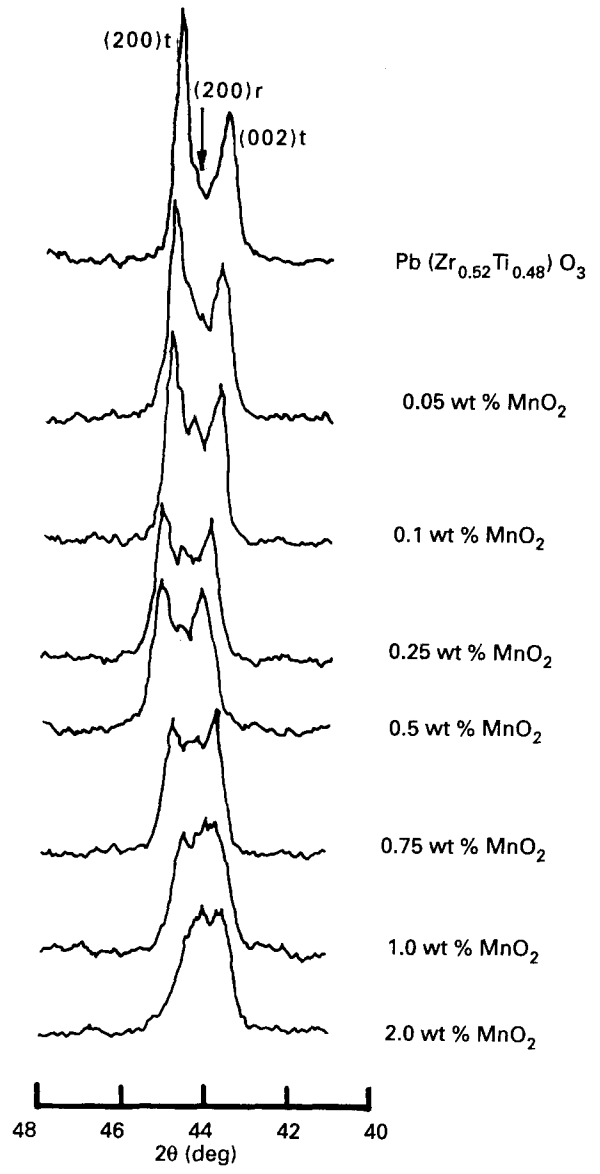

Figure 1 Profile of the diffraction lines $(0\,0\,2)_t$, $(2\,0\,0)_r$, $(2\,0\,0)_t$ for $Pb(Zr_{0.52}Ti_{0.48})O_3$ ceramics with MnO_2 addition.

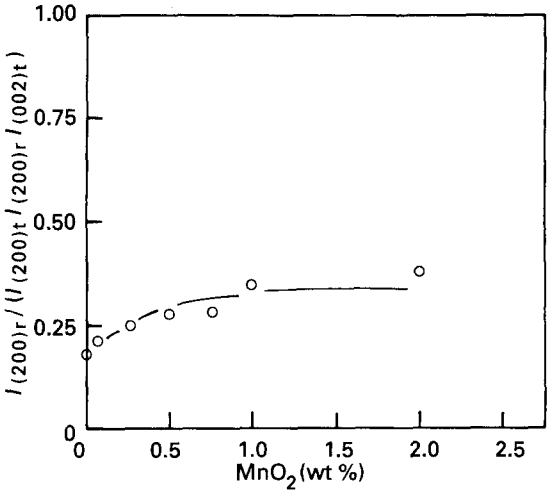

Figure 2 $I_{(2\,0\,0)r}/(I_{(2\,0\,0)t} + I_{(2\,0\,0)r} + I_{(0\,0\,2)t})$ variation with MnO_2 addition for $Pb(Zr_{0.52}Ti_{0.48})O_3$ ceramics

Ng and Alexander [13] reported the limit of solubility of MnO_2 in the PZT ceramics was about 2.5 mol % (0.677 wt %). This results from the stabilization effect of the rhombohedral phase by the substitution of

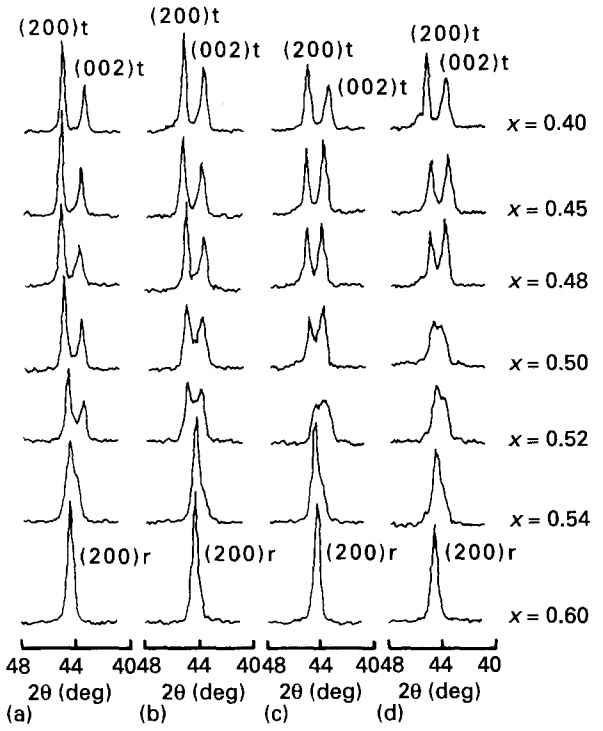

Figure 3 Profile of the diffraction lines, $(002)_t$, $(200)_r$, $(200)_t$ for MnO_2-doped $Pb(Zr_xTi_{1-x})O_3$ ceramics with zirconium concentration, x. (a) 0.0 wt % MnO_2, (b) 0.5 wt % MnO_2, (c) 1.0 wt % MnO_2, (d) 2.0 wt % MnO_2.

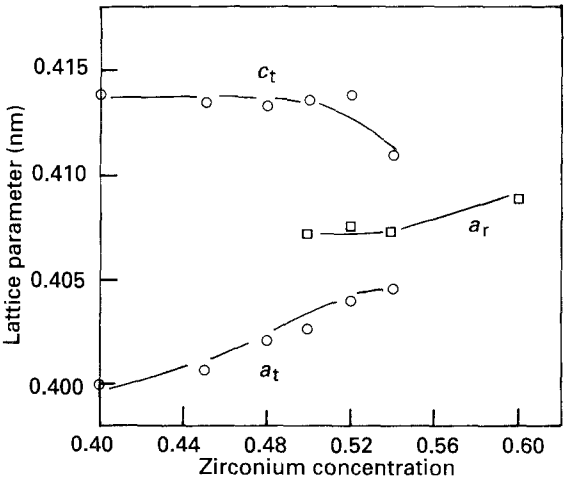

Figure 4 Variation of lattice parameter, a, c, for pure $Pb(Zr_xTi_{1-x})O_3$ ceramics with zirconium concentration, x.

manganese ions in the PZT lattice site [6, 7], and show good agreement with Weston *et al.*'s report [11], which discussed the effects of the addition of iron ions.

To investigate the distribution of MnO_2 additive in the PZT ceramics, XRD, SEM and electron microprobe examinations were conducted [6, 7]. As shown in Fig. 1, the XRD patterns do not indicate the existence of the second phase up to 3.0 wt % MnO_2-doped $Pb(Zr_{0.52}Ti_{0.48})O_3$ ceramics. The SEM and electron microprobe analyses indicate considerable heterogeneities for the $Pb(Zr_{0.52}Ti_{0.48})O_3$ ceramics with 5.0 wt % MnO_2 additive. However, those with less than 1.0 wt % MnO_2 additions are relatively homogeneous. These results are slightly consistent with the solubility limit indicated above.

Fig. 3 shows the variations of the (200) diffraction patterns with increasing zirconium concentration in the MnO_2-doped $Pb(Zr_xTi_{1-x})O_3$ ceramics. As the zirconium concentration increases, the patterns show a single peak due to phase transition to the rhombohedral, but the phase coexistence region shows three lines: $(002)_t$ and $(200)_t$ of the tetragonal phase, and $(200)_r$ of the rhombohedral phase. Moreover, the coexistence amount in the rhombohedral phase increases with increasing of MnO_2 as shown in Figs 1 and 2. Also, in Figs 1 and 3, the (200) reflection patterns of the pure $Pb(Zr_xTi_{1-x})O_3$ ($x = 0.52$, 0.54) ceramics show good agreement with those of Kakegawa's chemically precipitated PZT ceramics [2, 8]. This results from the carefully prepared conditions in this work to minimize the compositional fluctuation effect.

Fig. 4 shows the variation in lattice constant with increasing zirconium concentration in the pure $Pb(Zr_xTi_{1-x})O_3$ ceramics, and agreement with the results of Kakegawa *et al.* [2] and Turik *et al.* [1] can be seen. The continuous variation in lattice constant was due to the first-order transition of the morphotropic phase between the tetragonal and the rhombohedral phases, as reported by Nakamura [14].

In Fig. 4, a_t of the tetragonal phase increases, but c_t of the tetragonal phase does not change greatly with increasing zirconium concentration in the tetragonal region ($x \leqslant 0.50$). These results are due to the substitution by Zr^{4+} ion having a larger ionic radius than that of the Ti^{4+} ion, as reported by Sawaguchi [15]. However, in the phase coexistence region ($0.50 \leqslant x \leqslant 0.54$, $\Delta x \simeq 0.04$), a_t does not change greatly, but c_t decreases slightly, and a_r of the rhombohedral does not change significantly, as reported by Ari-gur and Benguigui [16, 17] and Kala [5]. The phase transition from the tetragonal phase to the rhombohedral phase takes place as a result of the change in concentration at constant temperature [3]. As reported by Isupov [3], this should take place by nucleus formation and there should be a concentration hysteresis [3, 18]. Therefore, as shown in Fig. 4, the lattice constant does not change significantly in the phase coexistence region. In this region, the relative coexisting amount of phase was determined by the lever rule [10].

Also in Fig. 4, the decrease of c_t in the coexistence region might result from the effect of decreasing c_t due to the phase transition to the rhombohedral. From Fig. 4, the width of the phase coexistence region can be estimated to be $\Delta x \simeq 0.04$, which shows approximate agreement with the results of Turik *et al.* [1] and Kala [5]. Kakegawa and Mohri [8] reported that the width of the morphotropic phase boundary region in the chemically precipitated PZT ceramics was confined within 1 mol % Zr($0.53 \leqslant x \leqslant 0.54$). The width of the phase coexistence region may not depend only on the homogeneity, but also on the external mechanical and electrical stresses, composition, sintering temperature and duration time, and the preparation method [1–5, 8, 9].

Fig. 5 shows the variation in lattice constant with increasing zirconium concentration in the 0.5 wt %

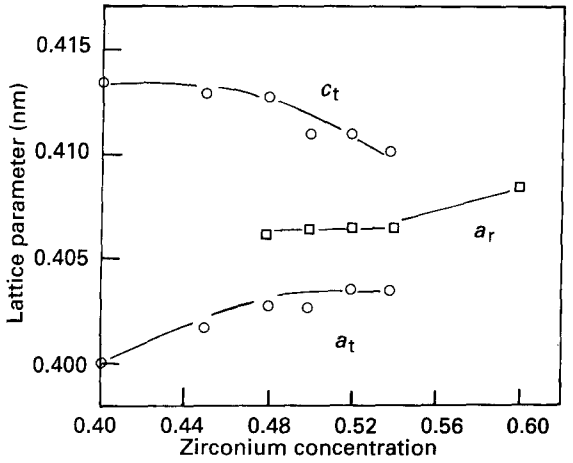

Figure 5 Variation of lattice parameter, a, c, for 0.5 wt % MnO_2-doped $Pb(Zr_xTi_{1-x})O_3$ ceramics with zirconium concentration, x.

MnO_2-doped $Pb(Zr_xTi_{1-x})O_3$ ceramics. The tendency is in good agreement with that of Fig. 4. However, the phase coexistence region was slightly moved to the tetragonal side ($0.48 \leqslant x \leqslant 0.54$, $\Delta x \simeq 0.06$) compared to that of the pure $Pb(Zr_xTi_{1-x})O_3$. This phenomenon is due to an increase of the coexistence amount of the rhombohedral phase with MnO_2 addition [1, 11], as shown in Fig. 2.

Fig. 6 shows the variations in tetragonality, relative coexistence amount of rhombohedral phase, dielectric constant, tan δ, coercive field, E_c, and remanent polarization, P_r, with increasing zirconium concentration for the pure $Pb(Zr_xTi_{1-x})O_3$ ceramics. As the zirconium concentration increases, the dielectric constant increases up to $x = 0.52$ owing to the effect of decreasing lattice distortion resulting from the decrease of the tetragonality in the tetragonal region. In the phase coexistence region ($0.50 \leqslant x \leqslant 0.54$), P_r increases abnormally up to $x = 0.54$ and then saturates. E_c and tetragonality also decrease abnormally up to $x = 0.54$.

Fig. 7 shows the variation in microstructure with increasing zirconium concentration for the 2.0 wt % MnO_2-doped $Pb(Zr_xTi_{1-x})O_3$ ceramics. No considerable change in microstructure with the variation of the composition can be detected. Table I shows the variation in apparent density with increasing zirconium concentration for the 0.5 wt % and 2.0 wt % MnO_2-doped $Pb(Zr_xTi_{1-x})O_3$ ceramics. The variation of apparent density is not distinctive with increasing zirconium concentration. Therefore, as shown in Fig. 7 and Table I, the characteristics of $Pb(Zr_xTi_{1-x})O_3$ ceramics with increasing zirconium concentration might be independent of their densities and microstructures. However, it might be abnormally influenced by the coexistence phenomena between the tetragonal and the rhombohedral phases with zirconium concentration, as shown in Fig. 6, which shows the abnormal property variations in the coexistence region with increasing zirconium concentration.

Fig. 8 shows the variation in the tetragonality, relative amount of coexistence of the rhombohedral phase, dielectric constant, tan δ, E_c, and P_r with increasing zirconium concentration for the 0.5 wt % MnO_2-doped $Pb(Zr_xTi_{1-x})O_3$ ceramics. Variation in the planar coupling factor, K_p, for the 0.5 wt %

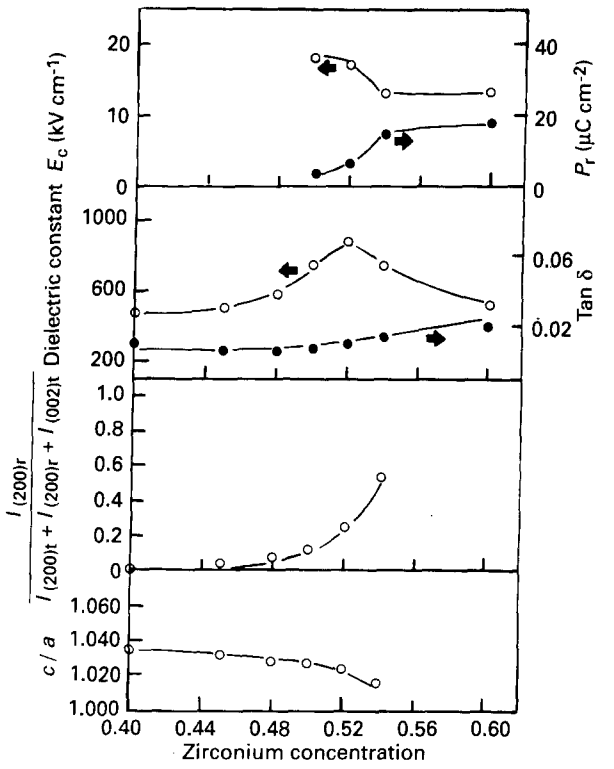

Figure 6 Variation of E_c, P_r, dielectric constant, tan δ, c/a, and $I_{(2\,0\,0)r}/(I_{(2\,0\,0)t} + I_{(2\,0\,0)r} + I_{(0\,0\,2)t})$ for pure $Pb(Zr_xTi_{1-x})O_3$ ceramics with zirconium concentration, x.

TABLE I Variation of apparent density for the 0.5 and 2.0 wt % MnO_2-doped $Pb(Zr_xTi_{1-x})O_3$ ceramics with zirconium concentration, x

Zirconium concentration	Apparent density (g cm^{-3})	
	0.5 wt % MnO_2	2.0 wt % MnO_2
0.40	7.732	7.694
0.45	7.731	7.707
0.48	7.753	7.695
0.50	7.751	7.669
0.52	7.787	7.707
0.54	7.752	7.617
0.60	7.754	7.695

MnO_2-doped $Pb(Zr_xTi_{1-x})O_3$ ceramics with zirconium concentration is shown in Fig. 9. The tendency in the variation is in good agreement with that in Fig. 6. However, the inflection point of the dielectric constant and abnormally changed point of E_c and P_r in the phase coexistence region shift to the lower zirconium concentration in proportion to MnO_2 addition. The relative amount of the coexistence of the rhombohedral phase increases with MnO_2 addition. Moreover, the variation patterns of dielectric constant show good agreement with those of K_p, as shown in Figs 8 and 9.

The tendencies in variation in Fig. 10 were in good agreement with those in Figs 6 and 8. In Figs 6, 8, and 10, the inflection points of the dielectric constant, and the abnormal variations in E_c and P_r appear in the phase coexistence region. However, there is no detectable change in either the apparent density or the microstructure, as shown in Fig. 7 and Table I. Therefore, these distinctive phenomena result from the

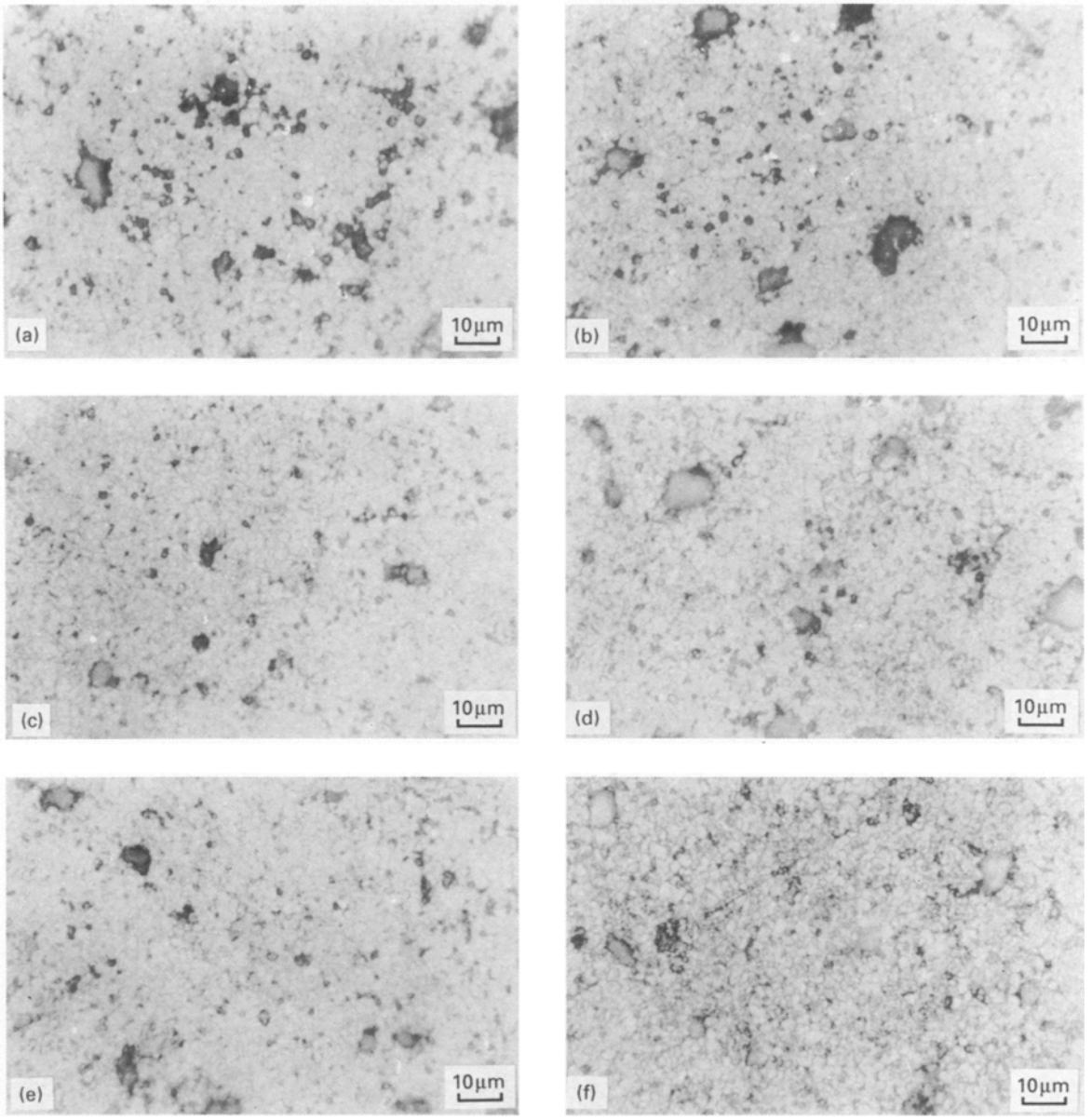

Figure 7 Optical micrographs for 2.0 wt % MnO_2-doped $Pb(Zr_xTi_{1-x})O_3$ ceramics with zirconium concentration, x: (a) 0.45, (b) 0.48, (c) 0.50, (d) 0.52, (e) 0.54, (f) 0.60.

phase coexistence between the tetragonal and rhombohedral phase.

As discussed in Figs 4 and 5, the width, Δx, of the phase coexistence region estimated from the variation in lattice constant was $\Delta x \simeq 0.04$ $(0.50 \leqslant x \leqslant 0.54)$ for the pure PZT ceramics and $\Delta x \simeq 0.06 (0.48 \leqslant x \leqslant 0.54)$ for the 0.5 wt % MnO_2-doped PZT ceramics. However, it is difficult to evaluate the MnO_2 addition effect on compositional fluctuation of the $Pb(Zr_xTi_{1-x})O_3$ ceramics. Owing to the linear dependency of intensity of the diffraction lines ($I_{(2\,0\,0)t}$, $I_{(0\,0\,2)t}$, $I_{(2\,0\,0)r}$) versus the zirconium concentration, x, in the phase coexistence region in Figs 6, 8, and 10, as reported by Hahn *et al.* [10] and Kala [5], the degree of compositional fluctuation for the pure and MnO_2-doped PZT ceramics was calculated from the least-square fitting curves [5, 9, 10].

Table II shows the relative amount of the rhombohedral phase, as shown in Figs 6, 8, and 10, and the calculated width and range of the phase coexistence for the $Pb(Zr_xTi_{1-x})O_3$ ceramics with MnO_2 additions. The data of the relative amount of the rhombohedral phase below 10% and above 70% were not considered in the calculation owing to some difficulties in estimation [10].

As shown in Table II, the width, Δx of the phase coexistence with MnO_2 addition was almost constant, and the phase coexistence region was slightly moved to the tetragonal side with MnO_2 addition, as discussed in Figs 1, 2 and 5, which show good agreement with the results of Weston *et al.* [11], Ouchi *et al.* [12], and Lucuta *et al.* [19]. These results indicate a negligible effect on compositional fluctuation of the PZT ceramics, owing to the homogeneous distribution of MnO_2 in this work, and the stabilization effect of the rhombohedral phase, owing to the substitution effect in the PZT lattice site, as discussed in Figs 1 and 2.

In Table II, the values of Δx are large compared with the values estimated from lattice parameter variations in Figs 4 and 5. These results show good agreement with Kala's report [5]. Kala [5] reported, for the 1.5 mol % (0.4 wt %) MnO_2-doped $Pb(Zr_xTi_{1-x})O_3$

TABLE II The calculated width, Δx, and range of the phase coexistence derived from the relative amount of the rhombohedral phase as shown in Figs 6, 8, and 10 by the least-squares fitting curves

Specimens	Relative amount of the rhombohedral phase in Figs 6, 8, and 10				Calculated coexistence range	Width (Δx)
	$x = 0.48$	$x = 0.50$	$x = 0.52$	$x = 0.54$		
$Pb(Zr_xTi_{1-x})O_3$	–	0.11	0.25	0.54	$0.493 \leqslant x \leqslant 0.582$	0.089
+ 0.5 wt % MnO_2	–	0.18	0.45	0.66	$0.485 \leqslant x \leqslant 0.568$	0.083
+ 1.0 wt % MnO_2	0.10	0.20	0.60	0.68	$0.476 \leqslant x \leqslant 0.562$	0.086

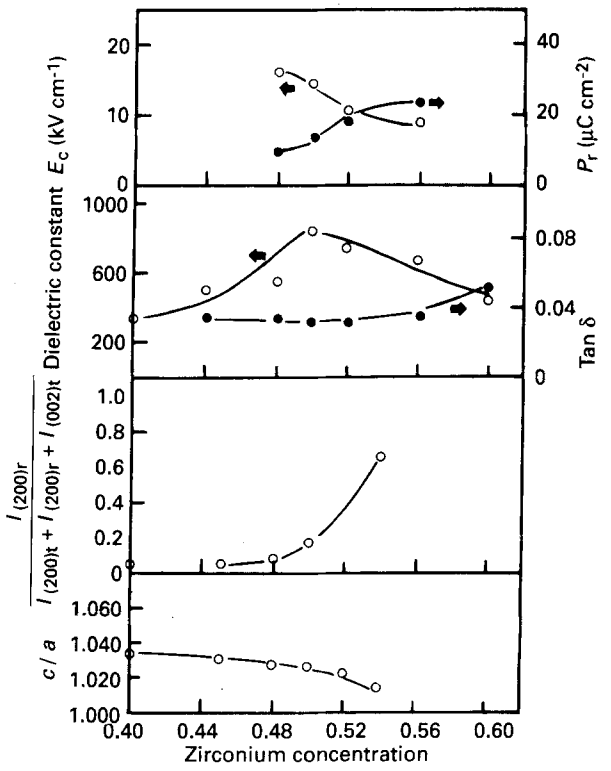

Figure 8 Variation of E_c, P_r, dielectric constant, tan δ, c/a, and $I_{(2\,0\,0)r}/(I_{(2\,0\,0)t} + I_{(2\,0\,0)r} + I_{(0\,0\,2)t})$ for 0.5 wt % MnO_2-doped $Pb(Zr_xTi_{1-x})O_3$ ceramics with zirconium concentration, x.

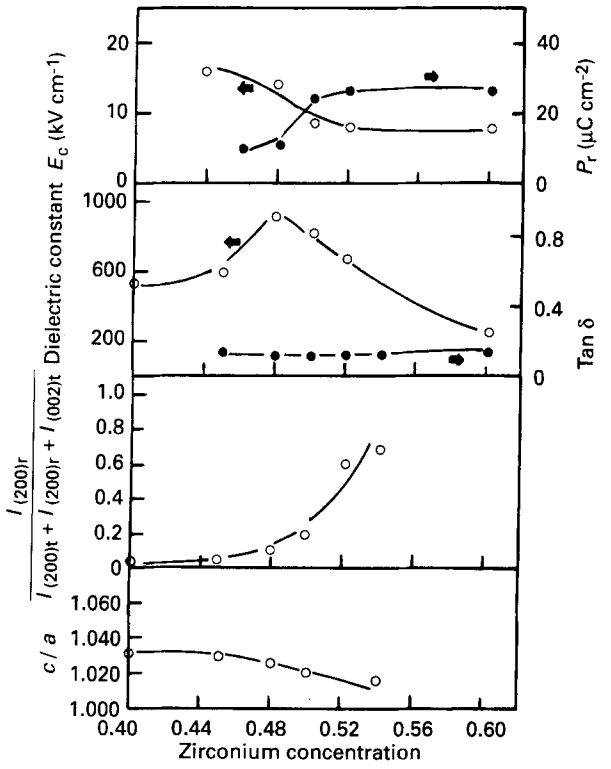

Figure 10 Variation of E_c, P_r, dielectric constant, tan δ, c/a, and $I_{(2\,0\,0)r}/(I_{(2\,0\,0)t} + I_{(2\,0\,0)r} + I_{(0\,0\,2)t})$ for 1.0 wt % MnO_2-doped $Pb(Zr_xTi_{1-x})O_3$ ceramics with zirconium concentration, x.

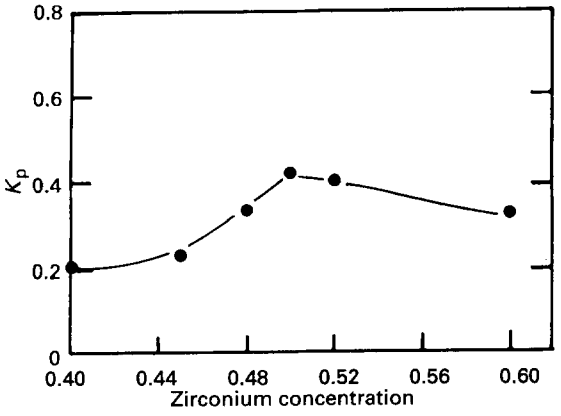

Figure 9 Variation of planar coupling factor, K_p, for 0.5 wt % MnO_2-doped $Pb(Zr_xTi_{1-x})O_3$ ceramics with zirconium concentration, x, at a poling field of 30 kV cm^{-1}.

ceramics, that Δx was estimated to be about $0.03 (0.52 \leqslant x \leqslant 0.55)$ from lattice parameter variations, but about $0.08 (0.48 \leqslant x \leqslant 0.56)$ from least-square fitting curves of the diffraction line intensities. These discrepancies between data calculated from the computed fitting curves and those estimated from variation patterns in the lattice constant might result from error factors due to the absence in the correction of estimating the X-ray intensities ($I_{(2\,0\,0)t}$, $I_{(0\,0\,2)t}$, $I_{(2\,0\,0)r}$).

In Figs 6, 8 and 10, the inflection points of dielectric constant appeared at the abnormally increasing region of the relative amount of the rhombohedral phase, and that of the variation of E_c and P_r. These phenomena were in good agreement with Fesenko *et al.*s report [20]. Hahn *et al.* [10] explained the behaviour of the dielectric constant and tan δ in the phase coexistence region as mixing rules. On the other hand, Mabud [9] assumed the possible existence of the rhombohedral phase region in the matrix of the tetragonal phase, or the tetragonal phase region in the matrix of the rhombohedral phase (different symmetry region, DSR [3]). Isupov [3] also reported the increasing effect, in the dielectric constant and piezoelectric constant, of movement of the interphase boundary of the region (DSR) because the spontaneous polarization directions were different from each other. Moreover, Isupov [3] reported that movement of these

phase boundaries was inhibited by a non-180° domain wall. In addition, Berlincourt and Krueger [21] reported that the amount of the non-180° domain increased with increasing relative amount of the rhombohedral phase. So, in the phase coexistence region, when the relative amount of rhombohedral phase is very small, the dielectric constant increases up to the inflection point, as shown in Figs 6, 8, and 10, due to increased mobility of these interphase boundaries.

When the relative amount of the rhombohedral phase increases as the zirconium concentration increases, the dielectric constant decreases due to the inhibition of movement of the DSR resulting from an increase in the number of non-180° domain walls, as reported by Isupov and Boudys [3, 22]. The phenomena of increasing P_r and decreasing E_c owing to an increase of the relative coexistence amount of the rhombohedral phase, resulted from an increase of the polarization-reversal effect [3] due to an increase of the relative amount of the rhombohedral phase.

4. Conclusion

In the phase coexistence region, the relative coexistence amount between the tetragonal and rhombohedral phases has a great influence on dielectric and piezoelectric properties, and the relative amount of the rhombohedral phase increases with increasing MnO_2 and zirconium.

In the coexistence region between the tetragonal and the rhombohedral phases, as the zirconium concentration increased, the dielectric constant and K_p increased up to a certain composition and then decreased. The inflection point of the dielectric constant shifted to a lower zirconium concentration in proportion to MnO_2 addition, owing to the substitution effect on the PZT lattice site.

References

1. A. V. TURIK, M. F. DUPRIYANOV, E. N. SIDORENKO and D. M. ZAITSEV, *Sov. Phys. Tech. Phys.* **25** (1980) 1251.
2. K. KAKEGAWA, J. MOHRI, S. SHIRASAKI and K. TAKAHASHI, *J. Am. Ceram. Soc.* **65** (1982) 515.
3. V. A. ISUPOV, *Ferroelectrics* **46** (1983) 217.
4. F. VASILU, P. GR. LUCUTA and F. CONSTANTINESCU, *Phys. Status Solidi (a)* **80** (1983) 637.
5. T. KALA, *ibid.* **78** (1983) 277.
6. J. S. KIM, K. H. YOON, B. H. CHOI and J. M. LEE, *J. Kor. Ceram. Soc.* **27** (1990) 187.
7. *Idem, ibid.* **28** (1991) 297.
8. K. KAKEGAWA and J. MOHRI, *Solid State Commun.* **24** (1977) 769.
9. S. A. MABUD, *J. Appl. Crystallogr.* **13** (1980) 211.
10. L. HAHN, K. UCHINO and S. NOMURA, *Jpn J. Appl. Phys.* **17** (1978) 634.
11. T. B. WESTON, A. H. WEBSTER and V. M. McNAMARA, *J. Am. Ceram. Soc.* **52** (1969) 253.
12. H. OUCHI, M. NISHIDA and S. HAYAKAWA, *ibid.* **49** (1966) 577.
13. Y. S. NG and S. M. ALEXANDER, *Ferroelectrics* **51** (1983) 81.
14. T. NAKAMURA, *Ceramics* **14** (1979) 894.
15. E. SAWAGUCHI, *Jpn J. Appl. Phys.* **8** (1953) 615.
16. P. ARI-GUR and L. BENGUIGUI, *J. Phys. D Appl. Phys.* **8** (1975) 1856.
17. *Idem, Solid State Commun.* **15** (1974) 1077.
18. V. A. ISUPOV, *Sov. Phys. Solid State* **16** (1975) 1370.
19. P. GR. LUCUTA, F. CONSTANTINESCU and D. BARB, *J. Am. Ceram. Soc.* **68** (1985) 533.
20. E. C. FESENKO, A. YA. DANTSIGER, L. A. RESNITCHENKO and M. F. KUPRIYANOV, *Ferroelectrics* **41** (1982) 137.
21. D. BERLINCOURT and H. A. KRUEGER, *J. Appl. Phys.* **30** (1959) 1804.
22. V. A. ISUPOV and M. BOUDYS, *Ferroelectrics* **41** (1982) 111.

Received 26 February
and accepted 20 August 1993